UTILISING SATELLITE IMAGERY AND DIGITAL DETECTION OF CLEAR CUTTINGS FOR TIMBER SUPPLY MANAGEMENT

Reija HAAPANEN,Anssi PEKKARINEN
Finnish Forest Research Institute
National Forest Inventory
Unioninkatu 40 A, 00170 Helsinki, Finland
reija.haapanen@metla.fi
anssi.pekkarinen@metla.fi

KEY WORDS: change detection, segmentation, multi-temporal, GIS

ABSTRACT

This paper presents an approach to detect clear cuttings by means of multitemporal satellite imagery. The process can be divided into three modules: image calibration, segmentation and detection of changes. In the method developed here, two images from different years were used and the changes were detected by means of the observed changes in the reflectance of the red channel. The output is a raster map with uniquely labelled clear cutting areas. The method was tested in the boreal forest of Southern Finland using Landsat TM data and evaluated by the help of visually delineated cutting areas and unchanged areas. The segment based detection of clear cuttings performed well and produced more meaningful clear cutting areas than a traditional pixel based approach. All the visually delineated reference areas of clear cuttings were found and more than 80% of their total area was correctly classified. At the same time errors in the classification of the total area of unchanged reference areas was less than 1%. The presented segment based method is thus recommended for updating clear cuttings in numerical forest resource data.

1 INTRODUCTION

Large-scale forest management requires up-to-date information about forest resources. In Finland, the multi-source National Forest Inventory (NFI) data is nowadays used in operational timber supply management. So far, this data has only provided information on forest resources. Especially in areas of active forestry, where several forest companies operate, these forest operations need to be monitored and mapped in order to avoid allocation of timber buying efforts to areas which have recently been cut. It is possible to base this updating on sequential multi-source inventories, but the interval of National Forest Inventories in Finland, 5-10 years, is too long for operational wood procurement. If the change detection is based on image data only, it may be more flexible in terms of costs and processing time. The drawback of this kind of method is that it can probably only detect drastic changes. If the goal is to detect only clear fellings, the use of image data may lead to satisfactory results.

Most of the conventional satellite image based change detection approaches operate pixel-by-pixel or by pixel blocks. If difference images are applied, pixel level approaches are, however, very sensitive to image noise and errors in image registration. One possibility to avoid this phenomenon is to use some kind of pre-defined detection units. These units could, for example, result from visual stand delineation for forest management planning. However, the real operations in the forest seldom follow these stand boundaries and the use of them in change detection is somehow doubtful. If the detection units are determined on the basis of the actual image data these kinds of problems can be avoided. Therefore, the change detection in this work was carried out by image segments.

2 MATERIALS

The image material consisted of two overlapping Landsat TM 5 images from different years; one acquired on June 3, 1992, path 187, row 17 and the other on June 22, 1998, path 187 floated. Both of the images contained a lot of clouds, cirrostrati and cumulus. Therefore a subset of the whole area covered by the imagery (as cloudless as possible) was used in this study. The size of the subset is 59 km x 59 km and it is situated in the Forestry Centres of Southern Savo and Kymi (figure 1). The images were independently rectified to the Finnish Uniform co-ordinate system using the nearest neighbour resampling and a second order polynomial model. The output pixel size was 25 metres. The RMS-error of the rectification model for the earlier image was 0.82 pixels and for the later image 0.46 pixels. The thermal channels (TM6)

were excluded. Topographic normalization was performed with the lambertian reflection model to reduce the topografic effect in digital imagery. The characteristics of the channels of the images are in table 1. Image X and Y co-ordinates and digital elevation model (DEM) were added to the dataset to test whether they could improve the calibration model. The co-ordinate and DEM channels were linearly scaled to a range of 0-50. Furthermore, a simple water mask was constructed as it appeared to be useful in the process. A pixel was considered to be water if the DN of channel TM4 (near-infrared) was less than that of channel TM3 (red) in either of the two images (Häme et al. 1998).

The results of the clear cutting detections were also compared to the area estimate calculated on the basis of the field plots of the 9th NFI. The inventory covered over one half of the study area in 1998, which is also the acquisition year of the later image. The amount of non-water field plots on the studied imagery was 569.

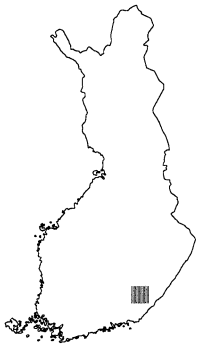

Figure 1: Location of the test area within the borders of Finland

Channel	TM92			TM98		
	mean	std	median	mean	std	median
TM1	82.04	8.30	81.00	67.48	7.13	67.00
TM2	33.56	5.11	33.00	26.92	4.20	26.00
TM3	30.82	7.42	29.00	22.59	5.56	22.00
TM4	73.24	19.49	70.00	77.25	24.81	72.00
TM5	65.38	23.92	60.00	55.64	19.52	52.00
TM7	26.89	13.47	24.00	18.99	7.54	18.00

Table 1: Characteristics of the channels in the original image data sets. Water areas excluded.

3 METHODS

Two methods that rely on unsupervised classification, image segmentation and Landsat TM image data were tested in the detection of clear cuts. Instead of traditional pixel-by-pixel (PBP) approaches, both the relative calibration of the images and the detection of clear cuts were based on image segments. The results of the segment based methods were compared to a PBP approach and evaluated by means of comparison to visually detected clear cutting and unchanged reference areas.

3.1 Image segmentation

Two image segmentation schemes were applied: the "Segmentation with directed trees"-algorithm (NG) (Narendra and Goldberg 1980) and a segmentation based on ISODATA clustering and labelling of connected components (CCL). Two different segmentations were derived with both methods: segmentations based on the multi-temporal image data (12 TM channels), DEM and co-ordinate data, and segmentations based on the image data of the later point of time only (6 TM channels). The segmentations of the multi-temporal datasets were applied in the construction of relative calibration models and the other segmentations in the actual detection of clear cuttings.

The NG algorithm has been used in many multi-source forest inventory studies (Hagner 1990, Häme 1991, Tomppo 1992, Parmes 1992, Olsson 1994). One of the main benefits of the algorithm is that it combines features from both edge and region based segmentation methods. At the same time, it avoids some of their drawbacks. The algorithm starts by dividing an image into edge and plateau points. This task is carried out by means of an edge and a gradient operator and a simple threshold value t. The mean edge strength e for image point $I(i,j)$ was defined in the 8-neighbourhood (N_8) of $I(i,j)$. The equation 1 was applied to the original grey values ($g_c(i,j)$) of all channels (c). The gradient operator was the same as in the original work of Narendra and Goldberg (1980) and can be found in equation 2. After the definition of the gradient, each image point is considered a plateau ($|G(i,j)| \leq t$) or an edge pixel.

$$e(i,j) = \frac{\sum_{c=1}^{nbr}(\sum |g_c(i,j) - g_c(k,l)|)}{nbr} \quad (k,l) \in N_8(i,j) \tag{1}$$

where

nbr = number of channels.

$$G(i,j) = \max[e(i,j) - e(k,l)] \quad (k,l) \in N_8(i,j) \tag{2}$$

The next step is the actual image segmentation which is carried out by two sequential passes over the image. During the first pass, all edge pixels are marked as root pixels ($G(i,j) < 0$) or linked to the direction of the weakest edge. During the second pass, all the plateau points are arbitrarily linked to the pixels of the same plateau. The formation of directed cycles is prohibited. If a plateau element cannot be linked to any of the neighbouring elements of the same plateau, it is considered a root pixel. Finally, all the root pixels are labelled and all the other pixels of an image are assigned the label of the root pixel of the directed tree they belong to. More detailed description of the algorithm can be found in Narendra and Goldberg (1980) or Tomppo (1992).

The other tested segmentation method is based on ISODATA clustering and labelling of connected components of the resulting output image. The number of clusters applied was 40, and the iterative clustering algorithm was run until 95% of the pixels remained in the same cluster during two sequential iterations. The result of the clustering was turned into segmentation by means of a sequential connected component labelling -algorithm (CCL)(see Jain et al. 1995). The 8-neighbourhood was applied. The connectivity was defined as follows: an image point $I(i,j)$ is connected to another image point $I(k,l)$ if $I(k,l) \in N_8(i,j)$ and $C(i,j) = C(k,l)$, where C is the label of the ISODATA cluster.

The results of both the segmentations were fine-tuned by means of the nearest neighbour region merging. All segments smaller than 4 pixels were merged to their spectrally nearest neighbouring segment. Euclidean distance measure was applied. The means and standard deviations of the segments were used in the distance calculation.

3.2 Relative calibration

The earlier image was radiometrically calibrated to the later image with relative regression calibration to reduce the atmospheric effects and changes due to normal growth. In order to take the different nature of the NG and ISOCCL segmentations into account, the calibration models for the change detection tests were based on the same segmentation method that was used to define the change detection units.

In all, six different calibration models were built. In the first model (model 1), the NG segment mean values were used in the construction of the first-phase relative regression calibration model. The model was a multiple regression model where the segment mean value of the later image was the response variable and the segment means of the earlier image, co-ordinates and DEM were the independent variables. In the second model (model 2), the ISOCCL segment mean values were used. The inverse variance of the segment intensities of the earlier image was used as a weight factor during the estimation of the parameters. Therefore, homogenous segments were given more weight in the parameter estimation (e.g. Varjo 1996). Both the the third model (model 3) and the fourth model (model 4) were simple band to band regression models, the difference being that model 3 was based on NG segment means and model 4 on ISOCCL segment mean values. In models 5 and 6, NG and ISOCCL segment mean values were (respectively) used to construct multiple regression models based on all bands of the earlier image (e.g. Olsson 1994). All the models were constructed separately for each band.

At the second phase of the calibration, the outliers of the first-phase model were removed from the material and the model was rebuilt. An observation was considered an outlier if its residual was more than twice the RMS-error of the image channel. By detecting and excluding outliers, the effect of clouds, cloud shadows and changes in the landscape was excluded from the calibration model. (Varjo 1996).

The band level co-efficients of determination of each of the constructed models are shown in table 2 and the RMS-errors are in shown table 3. Since the use of multiple bands as independent variables did not significantly improve the model, the more straightforward models (1 and 2) were chosen. The characteristics of the channels of the output images of models 1 and 2 are presented in table 4.

	Model 1	Model 2	Model 3	Model 4	Model 5	Model 6
TM1	0.69	0.72	0.69	0.72	0.65	0.71
TM2	0.59	0.55	0.59	0.55	0.62	0.63
TM3	0.43	0.40	0.43	0.39	0.44	0.46
TM4	0.97	0.91	0.97	0.91	0.84	0.77
TM5	0.96	0.87	0.96	0.87	0.73	0.67
TM7	0.72	0.59	0.69	0.59	0.56	0.52

Table 2: R^2 values of different calibration procedures

	Model 1	Model 2	Model 3	Model 4	Model 5	Model 6
TM1	0.80	0.87	0.80	0.87	2.87	2.37
TM2	1.08	1.23	1.07	1.22	1.97	1.58
TM3	1.15	1.37	1.15	1.37	2.67	2.18
TM4	0.65	1.25	0.66	1.26	9.47	9.13
TM5	0.56	1.10	0.55	1.10	9.03	8.58
TM7	0.73	1.11	0.72	1.10	3.73	3.27

Table 3: RMS-errors of different calibration procedures

Channel	Model 1			Model 2		
	mean	std	median	mean	std	median
TM1	66.80	5.08	66.00	66.56	5.11	66.00
TM2	26.32	2.89	26.00	26.03	2.80	26.00
TM3	21.96	3.56	21.00	21.51	3.46	21.00
TM4	76.84	19.12	74.00	73.95	18.93	71.00
TM5	56.73	13.99	54.00	52.68	14.02	50.00
TM7	18.42	5.23	18.00	17.36	5.08	16.00

Table 4: Characteristics of the TM channels of the calibrated data sets

3.3 Change detection

The detection of clear cuttings could be based on many alternative spectral features (e.g. Häme 1991, Olsson 1994, Varjo 1996, Varjo 1997). Our original purpose was to adapt the clear cutting detection part of an elegant four-field change type recognition algorithm presented in a recent study by Häme et al. (1998) and to modify it to a segment level approach. In the suggested technique, the areas that had undergone one of the four change types were recognised by means of a biomass index and NDVI. The decrease in the biomass implied change types of "General decline" and "Conifer decline", and the change in the NDVI was used as an indicator of the amount of broadleaf species. Thus, the detection of clear cuttings could have been based on the change type and change magnitude (CHMG) defined as Euclidean distance between the spectral bands of the image sets. Our experiences, however, reveal that the detection of clear cuttings based on this kind of change type and change magnitude thresholding does not work properly with the tested segment based approaches. First, the change type detection based on the signs of the change in NDVI and biomass index is very sensitive to errors in image calibration. Secondly, we observed that the CHMG yields to high values even in segments where no evidence of cuttings could be visually found. The use of the change magnitude of the segment mean values of the red channel (TM3) seemed a more robust way to detect the clear cuttings with both uncalibrated and calibrated datasets (figure 2). Thus, the thresholding by means of CHMG was not used. Instead, we applied a simple red change index (RCI) and thresholding based on the difference between the corrected segment mean values of red channel of the later and earlier image data sets:

$$RCI = \frac{\bar{x}^s_{t1}}{\bar{x}^s_{t-1}} \times \frac{\bar{x}_{t-1}}{\bar{x}_t}$$

where

RCI red change index
$\bar{x}_t^s$:segment mean of the channel TM3 in the later image
$\bar{x}_{t-1}^s$:segment mean of the channel TM3 in the earlier image
$\bar{x}_t$:global mean of the channel TM3 in the later image, water excluded
$\bar{x}_{t-1}$:global mean of the channel TM3 in the earlier image, water excluded

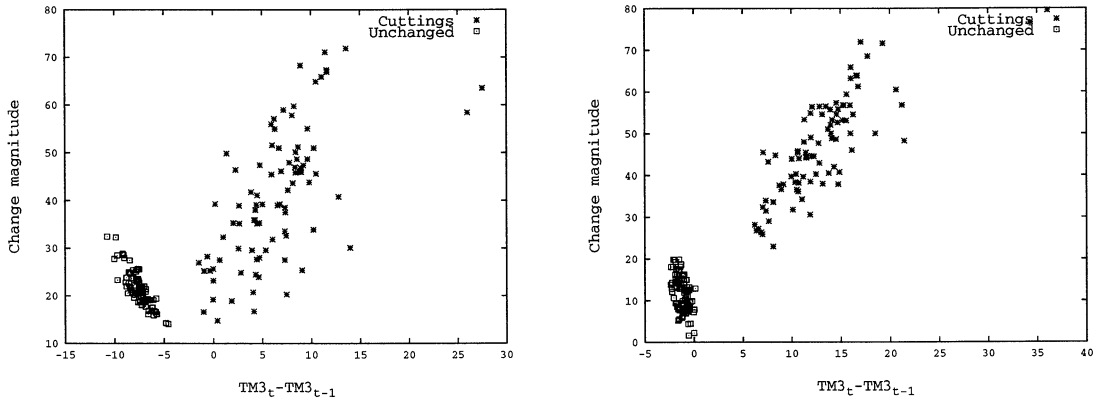

(a) Uncalibrated dataset

(b) NG calibrated dataset

Figure 2: The change magnitude of red channel ($TM3_t - TM3_{t-1}$) and CHMG of visually delineated cutting and unchanged areas.

Obviously, the values of RCI ought to be near 1 in the unchanged areas and significantly larger than 1 in the clear cutting areas.

The results of the segment and pixel based clear cutting detections were compared to reference material. This reference material was derived by means of manual delineation of clear cuts. The delineation was carried out by means of false-colour display of both image sets. The image set of the later point of time was swiped over the earlier one, and the borders of distinguishable clear cuttings were digitised on screen. Two independent delineations were carried out, and a union of the resulting cutting masks was used as reference material. The resulting number of spatially continuous clear cutting areas was 87 and their mean size was 5.0 hectares. In order to obtain an impression of the possible overestimation of clear cutting areas a mask for unchanged areas was also composed; each delineated polygon was moved to an area were no changes were detectable. The number of the areas logically equals the number of cutting areas, but due to the different rasterization process the average segment size was slightly smaller: 4.99 hectares.

4 RESULTS

The clear cutting detection succeeded well with both uncalibrated and calibrated imagery. With the uncalibrated image data sets, the best results were achieved with RCI values 1.2 and 1.4. Smaller thresholds lead to too large an estimate of the clear felling area. With a threshold value of 1.2 all the individual cutting areas were detected and less than 2% of the area of unchanged regions was erroneously classified (tables 5 and 6). Using threshold value 1.4 the optimal result was achieved with the unchanged areas, with both NG and ISOCCL methods. At the same time, the errors in the detected area of the cutting regions increased. With the most reasonable threshold values, the PBP method yielded to a significantly higher number of spatially continuous clear cutting areas and to a total area almost twice as large as by using the segment based methods (table 7).

	Method					
	PBP		NG		ISOCCL	
RCI threshold	nbr	area %	nbr	area %	nbr	area %
0.8	87	98.84	87	99.14	87	99.13
1.0	87	96.97	87	96.43	87	96.73
1.2	87	89.77	87	83.79	87	87.63
1.4	87	76.68	86	71.17	86	74.53

Table 5: The number of reference areas found by different change detection methods and the detected % of their total area. Uncalibrated imagery

	Method					
	PBP		NG		ISOCCL	
RCI threshold	nbr	area %	nbr	area %	nbr	area %
0.8	87	98.53	87	99.78	87	99.77
1.0	87	37.57	66	37.15	68	34.82
1.2	25	1.44	6	0.36	3	0.27
1.4	3	0.09	0	0.00	0	0.00

Table 6: The number of unchanged reference areas erroneously classified as clear cuttings and their area % of the total unchanged reference area. Uncalibrated imagery

	Method					
	PBP		NG		ISOCCL	
RCI threshold	nbr	area, ha	nbr	area, ha	nbr	area, ha
0.8	3484	204078.44	2516	213996.94	2581	212114.50
1.0	62911	104888.13	11341	101519.88	14562	97841.69
1.2	71356	28412.94	8681	15738.63	11004	18640.56
1.4	27514	10783.50	3637	6225.81	4830	7200.50

Table 7: The number and total area of spatially continuous clear cutting areas detected by different methods. Uncalibrated imagery

The best performance with the calibrated data sets was reached with the same threshold values as in the case of the uncalibrated data sets with all but PBP method using NG based calibrated imagery. The number of erroneously classified unchanged areas was generally smaller with the calibrated imagery, however, larger errors in the area estimates of the fellings were obtained (tables 8 and 9). With the calibrated datasets, the PBP method produced a remarkably higher number of spatially continuous clear cutting areas (table 10).

	Method							
	PBP				NG		ISOCCL	
	ISOCCL calibration		NG calibration					
RCI threshold	nbr	area %	nbr	area %	nbr	area	nbr	area %
0.8	87	99.04	87	93.44	87	99.14	87	99.13
1.0	87	96.61	87	76.65	87	93.13	87	95.70
1.2	87	87.39	85	42.23	87	80.53	87	84.03
1.4	87	67.80	70	18.11	82	61.82	85	66.14

Table 8: The number of reference areas found by different change detection methods and the detected % of their total area. Calibrated imagery

The percentage of regeneration fellings that took place between 1992 and 1998 in the 9th NFI was 4.22. About a half of the regeneration fellings were clear cuttings (2,28 % of the non-water field plots) and the rest were seeding fellings, shelterwood fellings or strip fellings. The clear felling area calculated by means of these numbers is 9522 ha (all final fellings) or 5144 ha (only clear fellings considered). The areas derived from different segmentation tests is closer to the pure clear felling area than that of all final fellings.

	Method							
	PBP				NG		ISOCCL	
	ISOCCL calibration		NG calibration					
RCI threshold	nbr	area %	nbr	area %	nbr	area %	nbr	area %
0.8	87	96.90	54	6.25	87	99.78	87	99.70
1.0	68	12.80	3	0.09	26	2.46	29	5.01
1.2	6	0.24	0	0.00	0	0.00	1	0.01
1.4	2	0.03	0	0.00	0	0.00	0	0.00

Table 9: The number of unchanged reference areas erroneously classified as clear cuttings and their area % of the total unchanged reference area. Calibrated imagery

	Method							
	PBP				NG		ISOCCL	
	ISOCCL calibration		NG calibration					
RCI threshold	nbr	area, ha	nbr	area, ha	nbr	area, ha	nbr	area, ha
0.8	3223	206313.31	96515	46023.13	2429	218282.69	2469	216658.87
1.0	79486	77252.50	27394	10730.94	12578	67526.13	16966	67141.44
1.2	45024	21345.31	9863	3346.56	7005	13515.94	9415	15924.63
1.4	20570	8230.44	3816	1226.87	2929	4861.81	4154	5986.69

Table 10: The number and total area of spatially continuous clear cutting areas detected by different methods. Calibrated imagery

5 CONCLUSIONS

The segment based change detection worked well with both data sets. Compared to the PBP approach, the number of the detected cuttings was smaller and the average size of the detected cuttings larger. This is due to the fact that segment based methods are not as sensitive to errors in image registration and random variation present in the image. The PBP method clearly overestimated the total area of cuttings and suggested a large number of cuttings of the size of one pixel. The result of the ISOCCL based change detection was slightly better than the NG based one. This is due to the fact, that the ISOCCL method does not take into account the spatial neighbourhood of a pixel. In the NG method, the segment borders are smoother and thus some fine details may be lost. If the detection result is considered from the viewpoint of timber supply management, the results of NG change detection may be best. It produces detection units of meaningful size and smooth borders. Thus, the resulting cutting mask is useful and compliant to any modern GIS.

In Finland, the NFI provides digital forest resource data that is easily importable to any raster-compliant GIS. Although the time interval of these inventories is quite long for timber supply management, its requirements may be satisfied by updating the digital forest resource maps with a cutting mask produced by means of clear cutting detection.

In the future it could be possible to store all the cuttings in a common database, but as the shared use of geographic information is still under process, the means of remote sensing can fill this need. The method presented here has proven to suit well for this purpose. Since no field data is needed, the costs of the method are also reasonable.

ACKNOWLEDGEMENTS

We would like to thank Dr. Jari Varjo for his encouragement during this work. The material and equipment used in this study was provided by the National Forest Inventory of the Finnish Forest Research Institute. This study was carried out in co-operation with the 'Forest in GIS' graduate school at the University of Helsinki, Department of Forest Resource Management.

REFERENCES

Hagner, O., 1990. Computer aided forest stand delineation and inventory based on satellite remote sensing. In Proceedings from SNS/IUFRO workshop in Umeå 26-28 February 1990: The usability of remote sensing for forest inventory and planning. Swedish University of Agricultural sciences. Remote sensing laboratory. Umeå.

Häme, T., 1987. Satellite image aided change detection. University of Helsinki, Department of Forest Mensuration and Management, Helsinki, Finland. Research notes 19, pp. 47-60.

Häme, T., 1988. Interpretation of forest changes from satellite scanner imagery. University of Helsinki, Department of Forest Mensuration and Management, Helsinki, Finland. Research notes 21, pp. 119-133.

Häme, T., 1991. Spectral interpretation of changes in forest using satellite scanner images. Acta Forestalia Fennica 222. 111 p.

Häme, T., Heiler, I., San Miguel-Ayanz J. 1997. An unsupervised change detection and recognition system for forestry. Int. J. Remote Sensing, 1998, vol 19, 6, pp. 1079-1099.

Jain, R., Kasturi, R. and Schunck, B. G. 1995. Machine Vision. McGraw-Hill, Inc. 549 p.

Narendra, P. and Goldberg, M. 1980. Image segmentation with directed trees. IEEE transactions on pattern analysis and machine intelligency Pami-2(2), pp. 185-191

Olsson, H., 1994. Monitoring of local reflectance changes in boreal forests using satellite data. Report 7, Department of biometry and forest management, Swedish University of agricultural sciences, Umeå, Sweden.

Parmes, E., 1992. Segmentation of Spot and Landsat satellite imagery. Photogrammetric Journal of Finland, 13, pp. 52-58.

Tomppo, E., 1992. Satellite image aided forest site fertility estimation for forest income taxation. Acta Forestalia Fennica 229, 70 p.

Varjo J., 1997. Change detection and controlling forest information using multi-temporal Landsat TM imagery. Acta Forestalia Fennica 258. 64 p.

Varjo J., 1996. Controlling continuously updated forest data by satellite remote sensing. Int. J. Remote Sensing, 1996, 17(1), pp. 43-67.

Varjo J. and Folving, S. 1997. Monitoring of forest changes using unsupervised methods: a case study from boreal forest on mineral soils. Scand. J. For. Res. 12, pp. 362-369.